Design of Optimized Microfluidic Devices for Viscoelastic Fluid Flow

M. A. Alves

Departamento de Engenharia Química, CEFT,
Faculdade de Engenharia da Universidade do Porto
Rua Dr. Roberto Frias, 4200-465 Porto, Portugal, mmalves@fe.up.pt

ABSTRACT

In this work we present a fully automated procedure for design of microfluidic devices with optimal performance. The proposed approach combines a finite-volume viscoelastic flow solver, an optimizer, and an automatic mesh generation and adaptation procedure.

The methodology can be used in the automatic search of the ideal shape of a given flow geometry, in order to achieve optimal performance. The procedure is fully automatic and general, and can be coupled with any computational fluid dynamics (CFD) solver. In this work we use a viscoelastic flow solver and apply the methodology in the design of two microfluidic devices with optimal performance under laminar flow conditions: (*i*) development of a microfluidic analogue of an electronic diode, which presents large anisotropic flow resistance in both flow directions; (*ii*) design of a microfluidic T-junction that generates a strong extensional flow with a nearly constant strain rate along the centerline.

Keywords: optimal shape design, viscoelastic fluid flow, extensional viscosity, microfluidics, rheometry

1 INTRODUCTION

Optimal shape design (OSD) methods are valuable numerical tools useful in diverse areas, such as fluid dynamics, structural mechanics or their combination [1]. The development of faster computers, with increased memory and storage capabilities, coupled with important developments in CFD methods allows currently the use of OSD solvers to analyze complex flow problems in acceptable computational times [2].

In this work we describe a fully automated procedure for the design of microfluidic devices with optimal performance. The proposed approach combines an in-house finite-volume viscoelastic flow solver [3,4] with the CONDOR optimizer [5] and an automatic mesh generation and adaptation procedure.

The proposed approach can be used in the automatic design of the *ideal* shape of a given geometry, in order to achieve optimal flow performance for a given goal. The numerical methodology is general, fully automatic, and can be coupled with any CFD solver. In this work we apply the OSD methodology in the optimization of two laminar flows of Newtonian and viscoelastic fluids.

In the first example, we design an efficient microfluidic analogue of an electronic diode, which presents significant anisotropic flow resistance in both flow directions [6,7]. The second test-case refers to the design of a microfluidic T-junction that generates a quasi-homogeneous extensional flow, which is useful for extensional rheometry measurements.

The remaining of this paper is organized as follows: in section 2 we present briefly the numerical method, following the presentation of the optimization results and the corresponding discussion. The paper ends with the main conclusions of the work.

2 NUMERICAL METHOD

The optimal shape design methodology employed in this investigation consists of three main components: (*i*) a fully-automated mesh generator program; (*ii*) a viscoelastic fluid flow solver [3,4]; (*iii*) an adequate optimizer. In this work we used the derivative-free CONDOR optimizer [5], which is easy to implement (works as a black box) and is freely available in the public domain. There are other freeware optimizers that can be used, such as the Global Optimization Platform (GOP) [8], or other proprietary, and in some cases costly, software.

In the proposed methodology, the shape of the geometry, to be optimized, is described by a set of design variables represented by a one-dimensional array, $\mathbf{X}$. The function defining the shape of the geometry can be simply a polynomial, or more interestingly a B-spline or a Bézier curve. In one of the examples presented in this work, we use cubic B-splines to describe the geometries, using a small number of control points (of the order of 10), which are stored in array $\mathbf{X}$.

Starting from an initial estimate of the design variables, $\mathbf{X}_0$ (supplied by the user), the initial mesh is automatically generated and the CFD simulation is conducted. After achieving a converged solution, the objective function (defined by the user, in order to maximize performance of the microfluidic channel) is computed from the numerical solution, and this value is sent to the CONDOR optimizer. This process is repeated for a number of design variable parameters, chosen by the CONDOR optimizer, until the optimal shape of the geometry is found. The optimization procedure described is illustrated in Figure 1. More details of the optimization technique used in this work can be found in Ref. [9], where a cross-slot geometry was successfully optimized numerically, with application in the measurement of the extensional viscosity of dilute polymeric solutions.

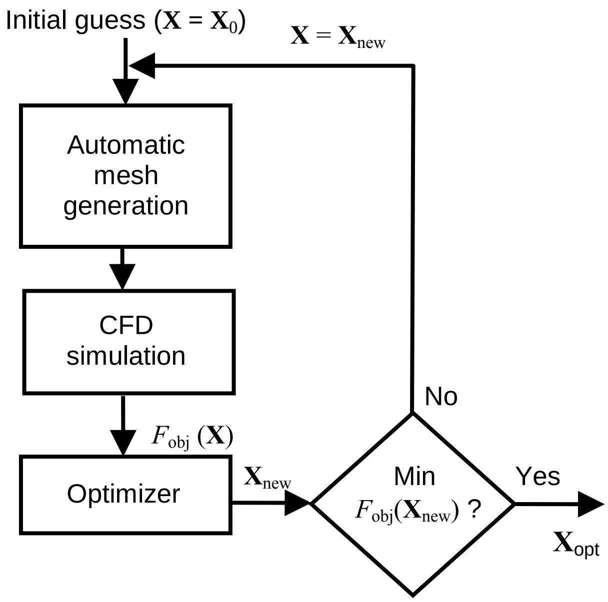

Figure 1: Illustration of the optimization algorithm (adapted from [9]).

An in-house finite-volume viscoelastic code [3,4] was used in this work. The equations solved by the CFD solver include the mass conservation of an incompressible fluid,

$$\nabla \cdot \mathbf{u} = 0 \tag{1}$$

and the momentum equation:

$$\rho\left(\frac{\partial \mathbf{u}}{\partial t} + \nabla \cdot \mathbf{u}\mathbf{u}\right) = -\nabla p + \nabla \cdot \boldsymbol{\tau}\,. \tag{2}$$

In Eqs. (1) and (2) p, $\mathbf{u}$ and $\boldsymbol{\tau}$ represent pressure, the velocity vector and the extra-stress tensor, respectively. To close the system of partial differential equations, an adequate evolution equation for the extra-stress tensor is also required. In this work we use the upper-convected Maxwell model, the simplest differential constitutive equation that represents viscoelastic behavior (but the more difficult to solve numerically):

$$\boldsymbol{\tau} + \lambda\left(\frac{\partial \boldsymbol{\tau}}{\partial t} + \nabla \cdot \mathbf{u}\,\boldsymbol{\tau}\right) = \eta\left(\nabla \mathbf{u} + \nabla \mathbf{u}^{\mathrm{T}}\right) + \lambda\left(\boldsymbol{\tau} \cdot \nabla \mathbf{u} + \nabla \mathbf{u}^{\mathrm{T}} \cdot \boldsymbol{\tau}\right). \tag{3}$$

In Eq. (3) λ and η represent the relaxation time and the constant shear viscosity of the fluid, respectively. The important limiting case of Newtonian fluid flow can also be simulated using the viscoelastic flow solver, by setting the relaxation time of the fluid equal to zero in Eq. (3), i.e. $\boldsymbol{\tau} = \eta(\nabla \mathbf{u} + \nabla \mathbf{u}^{\mathrm{T}})$. More details of the viscoelastic flow solver are presented in detail elsewhere [3,4,10]. The CFD code works as a black box within the optimization algorithm.

3 RESULTS AND DISCUSSION

In this section we present and discuss the results obtained using the OSD methodology described in the previous section.

3.1 Design of an Efficient Microfluidic Diode

The first example considers the design of a microfluidic channel that presents significant diodicity, defined as the ratio of flow rates in both flow directions (flow anisotropy) for the same applied pressure gradient.

In this example, the following *ad-hoc* general expression was used to describe the admissible shapes of the geometries:

$$y = \pm C_0 h \pm \sum_{j=1}^{\infty}\left[C_1 C_2^{j-1} \sin\left(j \frac{\pi}{2} \frac{x}{h}\right) \pm C_3 C_4^{j-1} \cos\left(j \frac{\pi}{2} \frac{x}{h}\right)\right] \tag{4}$$

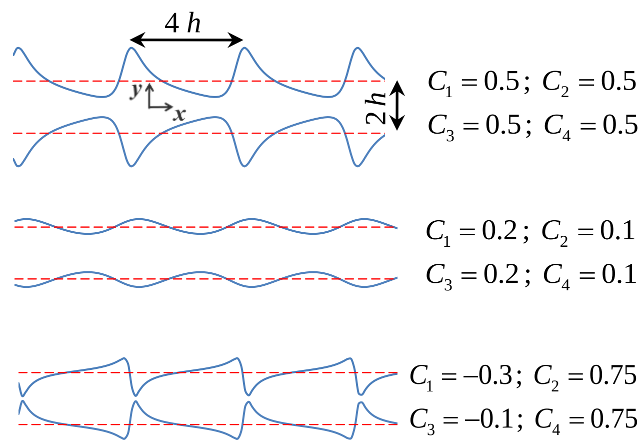

Figure 2: Illustration of several possible shapes of channels that can be generated using Eq. (4). In all cases $C_0 = 1$ was used, therefore the average width of the channel is $2\,h$ (shown by the dashed lines).

With only five adjustable parameters (C_i, $i = 0, 4$), Eq. (4) can describe a wide range of geometrical shapes, as illustrated in Figure 2. Increasing the number of adjustable parameters, and the complexity of the function, would result in more flexibility, but the complexity of the optimization problem would increase significantly, therefore Eq. (4) represents a good compromise between simplicity and efficiency. The average value of Eq. (4) is $\pm C_0 h$, therefore the average width of the microfluidic diode is $2C_0 h$. The remaining parameters control the amplitude of the sine and cosine terms (factors C_1 and C_3), and their decay rates (factors C_2 and C_4), as the frequencies increase with j. In a previous work [9] we used B-splines to describe the shape of the geometries, but otherwise stated the numerical procedure used in Ref. [9] is similar to the method used in the current work, therefore the details of the numerical procedure are not repeated here.

The OSD methodology was used to maximize the diodicity for Newtonian fluid flow at a small Reynolds number (Re = 10; results not shown) and for UCM fluid flow at a constant Deborah number of De = 0.2, in the creeping flow limit (Re = 0). The Deborah number is here defined as $De = \lambda U / H$, where U is the average velocity, in a section of width H (average width of the channel). In Figure 3 we illustrate the initial mesh used (straight channel with width H), and the optimal shape that maximizes the diodicity for the simulated conditions. In Figure 4 we show the variation of the pressure drop with the average velocity for the optimal geometry illustrated in Figure 3(b). The following parameters were considered in the numerical simulations: $\rho = 1000$ kg/m^3; $\eta = 0.010$ Pa s; $\lambda = 0.010$ s; $H = 100$ μm.

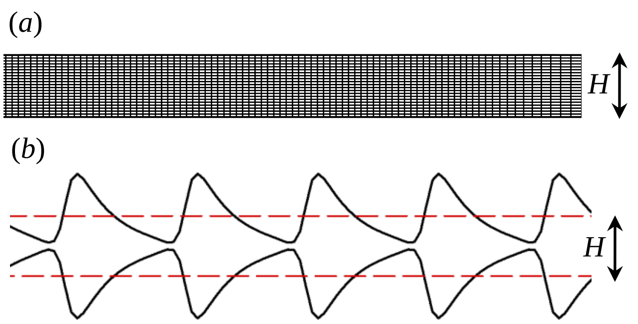

Figure 3: (a) Initial estimate and (b) optimized microfluidic diode.

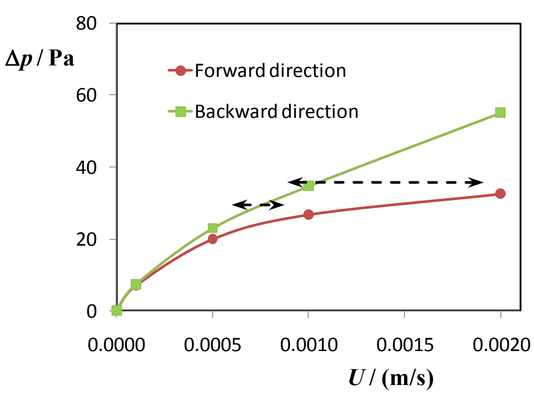

Figure 4: Influence of average velocity on the computed pressure drop in the optimized microfluidic rectifier illustrated in Figure 3(b).

For the higher pressure drops, the difference in the velocity (or flow rate) predicted for both flow directions becomes considerable, showing the high diodicity at larger De (or higher U). At $U = 0.002$ m/s we have $Re = 0.02$ (approximately creeping flow conditions) and $De = 0.2$, a situation very similar to the case considered in the optimization of the microfluidic diode.

3.2 Design of an Optimized Microfluidic T-Junction

The second example considers the design of a microfluidic T-junction that generates a quasi-homogeneous extensional flow, with a wide region where the fluid is subjected to a constant strain rate. Such microfluidic device can be used to estimate the extensional viscosity of the fluid, by measuring the stress field using birefringence techniques and the velocity field using micro-particle image velocimetry to estimate the corresponding strain rate. Figure 5 illustrates the control points used to define the shape of the geometries using cubic B-splines. The two extreme control points on each side are fixed, while the remaining points can be varied along the illustrated rays (dashed lines).

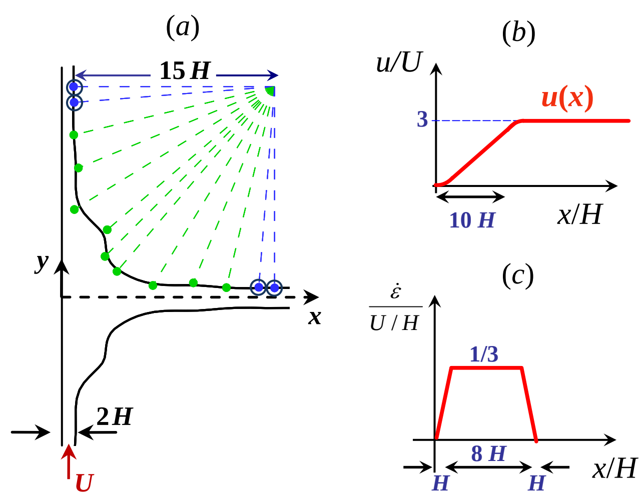

Figure 5: (a) Illustration of the control points that define the microfluidic T-junction and relevant variables. (b) Target velocity profile and (c) corresponding dimensionless strain rate profile along the centerline y = 0.

In this example, the objective function, to be minimized, was defined as $F_{obj} = \sum_i \left| (u_i - u_{i,\text{target}}) \right| \Delta x_i$ along the centerline (y = 0), where u_i is the computed x-velocity in computational cell i, with width Δx_i, and $u_{i,\text{target}}$ is the target velocity at point i, as illustrated in Figure 5(b).

In Figure 6 we illustrate the optimized geometries for Newtonian fluid flow and for a UCM fluid at Wi = 0.4. The Weissenberg number is defined as $Wi = \lambda \dot{\varepsilon}$. In both cases creeping flow conditions (Re = 0) were considered in the numerical simulations. The optimized geometries are very similar, which suggests that a universal microfluidic device can be designed, to be used for any fluid. Also, the agreement between the desired and computed velocity profiles is very good, indicating that the optimized geometries are efficient to provide a nearly constant strain rate profile, as required. In Figure 7 we present the computed streamlines and the contour plots of the streamwise normal stress calculated in the optimized geometries, showing the strong extensional flow generated in such microfluidic devices using viscoelastic fluids.

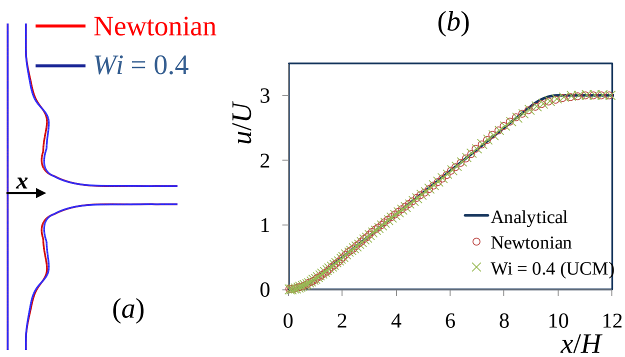

Figure 6: (*a*) Comparison between the optimal microfluidic T-junctions for Newtonian and viscoelastic (UCM model, *Wi* = 0.4) fluid flow. (*b*) Comparison between the target velocity profile and the computed profiles in the optimized geometries.

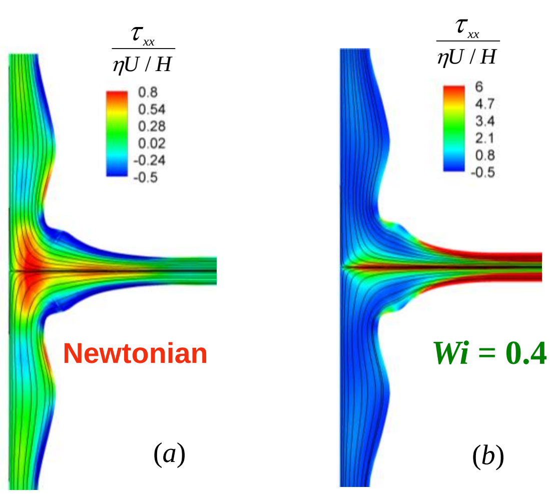

Figure 7: (*a*) Streamlines and contour plots of dimensionless axial normal stress computed in the optimal microfluidic T-junctions for Newtonian and viscoelastic fluid flow under creeping flow conditions.

4 CONCLUSIONS

An automatic algorithm for OSD studies of Newtonian and viscoelastic fluid flow was described and tested in the design of efficient microfluidic channels, including a microfluidic analogue of a diode and a T-junction for creating a quasi-homogeneous extensional flow. The algorithm combines a finite-volume viscoelastic code with an optimizer and an automatic mesh generation and adaptation procedure. The optimized geometries show enhanced flow behavior, illustrating the usefulness of the OSD methodology.

5 ACKNOWLEDGEMENTS

This work was funded by Fundação para a Ciência e a Tecnologia and FEDER through project PTDC/EQU-FTT/71800/2006.

REFERENCES

[1] B. Mohammadi and O. Pironneau, “Shape optimization in fluid mechanics”, Ann. Review Fluid Mech. 36, 255-279, 2004.

[2] Y. Tahara, S. Tohyama and T. Katsui, “CFD-based multi-objective optimization method for ship design”, Int. J. Num. Meth. Fluids, 52, 499-527, 2006.

[3] M.A. Alves, P.J. Oliveira and F.T. Pinho, “A convergent and universally bounded interpolation scheme for the treatment of advection”, Int. J. Num. Meth. Fluids, 41, 47-75, 2003.

[4] M.A. Alves, P.J. Oliveira and F.T. Pinho, "Benchmark solutions for the flow of Oldroyd-B and PTT fluids in planar contractions", J. Non-Newt. Fluid Mech. 110, 43-73, 2003.

[5] F.V. Berghen and H. Bersini, “CONDOR, a new parallel, constrained extension of Powell's UOBYQA algorithm: Experimental results and comparison with the DFO algorithm”, J. Comp. Appl. Math. 181, 157-175, 2005.

[6] A. Groisman and S.R. Quake, “A microfluidic rectifier: anisotropic flow resistance at low Reynolds numbers”, Phys. Rev. Lett. 92, 095401, 2004.

[7] P.C. Sousa, F.T. Pinho, M.S.N. Oliveira and M.A. Alves, “Efficient microfluidic rectifiers for viscoelastic fluid flow”, J. Non-Newt. Fluid Mech. 165, 652-671 (2010).

[8] L. Debiane, B. Ivorra, B. Mohammadi, F. Nicoud, T. Poinsot, A. Ern and H. Pitsch, “A low-complexity global optimization algorithm for temperature and pollution control of a complex chemistry flame”, Int. J. Comp. Fluid Dynamics, 20, 93-98, 2006.

[9] M.A. Alves, “Design of a cross-slot flow channel for extensional viscosity measurements”, Proc. XVth Int. Congress on Rheology – The Society of Rheology 80th annual meeting, Pts. 1 and 2, A. Co et al. (Eds.), Vol. 1027, pp. 240-242, American Institute of Physics, 2008.

[10] P.J. Oliveira, F.T. Pinho and G.A. Pinto, “Numerical simulation of non-linear elastic flows with a general collocated finite-volume method”, J. Non-Newt. Fluid Mech., 79, 1-43, 1998.